Achievement of target gain larger than unity in an inertial fusion experiment

H. Abu-Shawareb,[1] R. Acree,[2] P. Adams,[2] J. Adams,[2] B. Addis,[2] R. Aden,[2] P. Adrian,[3] B. B. Afeyan,[2,4] M. Aggleton,[1] L. Aghaian,[1] A. Aguirre,[2] D. Aikens,[2] J. Akre,[2] F. Albert,[2] M. Albrecht,[2] B. J. Albright,[5] J. Albritton,[2] J. Alcala,[1] C. Alday,Jr.,[1] D. A. Alessi,[2] N. Alexander,[1] J. Alfonso,[1] N. Alfonso,[1] E. Alger,[1] S. J. Ali,[2] Z. A. Ali,[6] A. Allen,[1] W. E. Alley,[2] P. Amala,[2] P. A. Amendt,[2] P. Amick,[2] S. Ammula,[2] C. Amorin,[2] D. J. Ampleford,[7] R. W. Anderson,[2] T. Anklam,[2] N. Antipa,[2] B. Appelbe,[8] C. Aracne-Ruddle,[2] E. Araya,[1] T. N. Archuleta,[5] M. Arend,[2] P. Arnold,[2] T. Arnold,[2] A. Arsenlis,[2] J. Asay,[7] L. J. Atherton,[2] D. Atkinson,[2] R. Atkinson,[1] J. M. Auerbach,[2] B. Austin,[1] L. Auyang,[2] A. A. S. Awwal,[2] N. Aybar,[2] J. Ayers,[2] S. Ayers,[2] T. Ayers,[9] S. Azevedo,[2] B. Bachmann,[2] C. A. Back,[1] J. Bae,[1] D. S. Bailey,[2] J. Bailey,[7] T. Baisden,[2] K. L. Baker,[2] H. Baldis[†,2] D. Barber,[1] M. Barberis,[2] D. Barker,[2] A. Barnes,[2] C. W. Barnes,[5] M. A. Barrios,[2] C. Barty,[2] I. Bass,[2] S. H. Batha,[5] S. H. Baxamusa,[2] G. Bazan,[2] J. K. Beagle,[2] R. Beale,[2] B. R. Beck,[2] J. B. Beck,[5] M. Bedzyk,[10] R. G. Beeler(II),[2] R. G. Beeler(III),[2] W. Behrendt,[2] L. Belk,[2] P. Bell,[2] M. Belyaev,[2] J. F. Benage,[7] G. Bennett,[7] L. R. Benedetti,[2] L. X. Benedict,[2] R. L. Berger,[2] T. Bernat,[2] L. A. Bernstein,[2,11,12] B. Berry,[1] L. Bertolini,[2] G. Besenbruch[†,1] J. Betcher,[9] R. Bettenhausen,[2] R. Betti,[10] B. Bezzerides[†,5] S. D. Bhandarkar,[2] R. Bickel,[2] J. Biener,[2] T. Biesiada,[2] K. Bigelow,[13] J. Bigelow-Granillo,[13] V. Bigman,[7] R. M. Bionta,[2] N. W. Birge,[5] M. Bitter,[14] A. C. Black,[2] R. Bleile,[2] D. L. Bleuel,[2] E. Bliss,[2] E. Bliss,[2] B. Blue,[2] T. Boehly,[10] K. Boehm,[1] C. D. Boley,[2] R. Bonanno,[2] E. J. Bond,[2] T. Bond,[2] M. J. Bonino,[10] M. Borden,[2] J.-L. Bourgade,[15] J. Bousquet,[1] J. Bowers,[2] M. Bowers,[2] R. Boyd,[2] D. Boyle,[2] A. Bozek,[1] D. K. Bradley,[2] K. S. Bradley,[5] P. A. Bradley,[5] L. Bradley,[1] L. Brannon,[1] P. S. Brantley,[2] D. Braun,[2] T. Braun,[2] K. Brienza-Larsen,[6] R. Briggs,[2] T. M. Briggs,[2] J. Britten,[2] E. D. Brooks,[2] D. Browning,[2] M. W. Bruhn,[2] T. A. Brunner,[2] H. Bruns,[2] G. Brunton,[2] B. Bryant,[2] T. Buczek,[10] J. Bude,[2] L. Buitano,[16] S. Burkhart,[2] J. Burmark,[2] A. Burnham,[2] R. Burr,[2] L. E. Busby,[2] B. Butlin,[2] R. Cabeltis,[1] M. Cable,[2] W. H. Cabot,[2] B. Cagadas,[1] J. Caggiano,[2] R. Cahayag,[1] S. E. Caldwell,[5] S. Calkins,[16] D. A. Callahan,[17] J. Calleja-Aguirre,[1] L. Camara,[2] D. Camp,[2] E. M. Campbell,[10] J. H. Campbell,[2] B. Carey,[2] R. Carey,[2] K. Carlisle,[2] L. Carlson,[1] L. Carman,[2] J. Carmichael,[1] A. Carpenter,[2] C. Carr,[2] J. A. Carrera,[2] D. Casavant,[2] A. Casey,[2] D. T. Casey,[2] A. Castillo,[1] E. Castillo,[1] J. I. Castor[†,2] C. Castro,[2] W. Caughey,[1] R. Cavitt,[2] J. Celeste,[2] P. M. Celliers,[2] C. Cerjan,[2] G. Chandler,[7] B. Chang,[2] C. Chang,[2] J. Chang,[2] L. Chang,[2] R. Chapman,[10] T. D. Chapman,[2] L. Chase,[2] H. Chen,[2] H. Chen,[1] K. Chen,[1] L.-Y. Chen,[2] B. Cheng,[5] J. Chittenden,[8] C. Choate,[2] J. Chou,[2] R. E. Chrien,[5,2] M. Chrisp,[2] K. Christensen,[2] M. Christensen,[2] N. S. Christiansen,[5] A. R. Christopherson,[2] M. Chung,[1] J. A. Church,[2] A. Clark,[1] D. S. Clark,[2] K. Clark,[1] R. Clark,[2] L. Claus,[7] B. Cline,[2] J. A. Cline,[2] J. A. Cobble,[5] K. Cochrane,[7] B. Cohen,[2] S. Cohen,[2] M. R. Collette,[2] G. W. Collins,[10] L. A. Collins,[5] T. J. B. Collins,[10] A. Conder,[18] B. Conrad,[2] M. Conyers[†,1] A. W. Cook,[2] D. Cook,[16] R. Cook,[2] J.C. Cooley,[5] G. Cooper,[7,19] T. Cope,[2] S. R. Copeland,[2] F. Coppari,[2] J. Cortez,[13] J. Cox,[2] D. H. Crandall,[16] J. Crane,[2] R. S. Craxton,[10] M. Cray,[5] A. Crilly,[8] J. W. Crippen,[1] D. Cross,[2] M. Cuneo,[7] G. Cuotts,[2] C. E. Czajka,[2] D. Czechowicz,[1] T. Daly,[2] P. Danforth,[2] C. Danly,[5] R. Darbee,[2] B. Darlington,[2] P. Datte,[1] L. Dauffy,[2] G. Davalos,[2] S. Davidovits,[2] P. Davis,[16] J. Davis,[2] S. Dawson,[2] R. D. Day,[5] T. H. Day,[5] M. Dayton,[2] C. Deck,[1] C. Decker,[2] C. Deeney,[16] K. A. DeFriend,[5] G. Deis,[2] N. D. Delamater,[5] J. A. Delettrez,[10] R. Demaret,[2] S. Demos,[2] S. M. Dempsey,[2] R. Desjardin,[2] T. Desjardins,[5] M. P. Desjarlais,[7] E. L. Dewald,[2] J. DeYoreo,[2] S. Diaz,[1] G Dimonte,[2,5] T. R. Dittrich,[2] L. Divol,[2] S. N. Dixit,[2] J. Dixon,[2] A. Do,[2] E. S. Dodd,[5] D. Dolan,[7] A. Donovan,[2] M. Donovan,[16] T. Döppner,[2] C. Dorrer,[10] N. Dorsano,[1] M.R. Douglas,[5] D. Dow,[9] J. Downie,[2] E. Downing,[2] M. Dozieres,[1] V. Draggoo,[2] D. Drake,[16] R. P. Drake,[2,20] T. Drake,[1] G. Dreifuerst,[2] O. Drury,[2] D. F. DuBois,[5] P. F. DuBois,[2] G. Dunham,[7] M. Durocher,[5] R. Dylla-Spears,[2] A. K. L. Dymoke-Bradshaw,[21] B. Dzenitis,[2] C. Ebbers,[2] M. Eckart,[2] S Eddinger,[1] D. Eder,[2] D. Edgell,[10] M. J. Edwards,[2] P. Efthimion,[14] J. H. Eggert,[2] B. Ehrlich,[2] P. Ehrmann,[2] S. Elhadj,[2] C. Ellerbee,[2] N. S. Elliott,[2] C. L. Ellison,[2] F. Elsner,[1] M. Emerich,[1] K. Engelhorn,[1] T. England,[7] E. English,[2] P. Epperson,[2] R. Epstein,[10] G. Erbert,[2] M. A. Erickson,[2] D. J. Erskine,[2] A. Erlandson,[2] R. J. Espinosa,[1] C. Estes,[2] K. G. Estabrook[†,2] S. Evans,[5] A. Fabyan,[1] J. Fair,[2] R. Fallejo,[2] N. Farmer,[1] W. A. Farmer,[2] M. Farrell,[1] V. E. Fatherley,[5] M. Fedorov,[2] E. Feigenbaum,[2] T. Fehrenbach,[22] M. Feit[†,2] B. Felker,[2] W. Ferguson,[2] J. C. Fernandez,[5] A. Fernandez-Panella,[2] S. Fess,[1] J. E. Field,[2] C. V. Filip,[2] J. R. Fincke,[5] T. Finn,[16] S.M. Finnegan,[5] R. G. Finucane,[2] M. Fischer,[2] A. Fisher,[2] J. Fisher,[2] B. Fishler,[2] D. Fittinghoff,[2] P. Fitzsimmons,[1] M. Flegel,[2] K. A. Flippo,[5] J. Florio,[1] J. Folta,[2] P. Folta,[2] L. R. Foreman[†,5] C. Forrest,[10] A. Forsman,[1] J. Fooks,[1] M. Foord,[2] R. Fortner,[2] K. Fournier,[2] D. E. Fratanduono,[2] N. Frazier,[16] T. Frazier,[2] C. Frederick,[1] M. S. Freeman,[5] J. Frenje,[3] D. Frey,[1] G. Frieders,[2] S. Friedrich,[2] D. H. Froula,[10] J. Fry,[2] T. Fuller,[1] J. Gaffney,[2] S. Gales,[23] B. Le Galloudec,[2] K. K. Le Galloudec,[2] A. Gambhir,[2] L. Gao,[14] W. J. Garbett,[23] A. Garcia,[1] C. Gates,[2] E. Gaut,[1]

P. Gauthier,[15] Z. Gavin,[1] J. Gaylord,[2] M. Geissel,[7] F. Génin,[2] J. Georgeson,[7] H. Geppert-Kleinrath,[5] V. Geppert-Kleinrath,[5] N. Gharibyan,[2] J. Gibson,[1] C. Gibson,[1] E. Giraldez,[1] V. Glebov,[10] S. G. Glendinning,[2] S. Glenn,[2] S. H. Glenzer,[2,18] S. Goade,[1] P. L. Gobby,[5] S. R. Goldman,[5] B. Golick,[2] M. Gomez,[7] V. Goncharov,[10] D. Goodin,[1] P. Grabowski,[2] E. Grafil,[2] P. Graham,[23] J. Grandy,[2] E. Grasz,[2] F. R. Graziani,[2] G. Greenman†,[2] J. A. Greenough,[2] A. Greenwood,[1] G. Gregori,[24] T. Green,[2] J. R. Griego,[5] G. P. Grim,[2] J. Grondalski,[2] S. Gross,[13] J. Guckian,[9] N. Guler,[25] B. Gunney,[2] G. Guss,[2] S. Haan,[2] J. Hackbarth,[1] L. Hackel,[2] R. Hackel,[2] C. Haefner,[2,26,27] C. Hagmann,[2] K. D. Hahn,[2] S. Hahn,[2] B. J. Haid,[2] B. M. Haines,[5] B. M. Hall,[2] C. Hall,[7] G. N. Hall,[2] M. Hamamoto,[2] S. Hamel,[2] C. E. Hamilton,[5] B. A. Hammel,[2] J. H. Hammer,[2] G. Hampton,[2] A. Hamza,[2] A. Handler,[2] S. Hansen,[7] D. Hanson,[7] R. Haque,[2] D. Harding,[10] E. Harding,[7] J. D. Hares,[21] D. B. Harris,[5] J. A. Harte,[2] E. P. Hartouni,[2] R. Hatarik,[2] S. Hatchett,[2] A. A. Hauer,[5] M. Havre,[1] R. Hawley,[2] J. Hayes,[1] J. Hayes†,[2] S. Hayes,[2] A. Hayes-Sterbenz,[5] C. A. Haynam,[2] D. A. Haynes,[5] D. Headley,[7] A. Heal,[2] J. E. Heebner,[2] S. Heerey,[2] G. M Heestand†,[2] R. Heeter,[2] N. Hein,[1] C. Heinbockel,[1] C. Hendricks,[2] M. Henesian,[2] J. Heninger,[2] J. Henrikson,[2] E. A. Henry,[2] E. B. Herbold,[2] M. R. Hermann,[2] G. Hermes,[2] J. E. Hernandez,[2] V. J. Hernandez,[2] M. C. Herrmann,[2] H. W. Herrmann,[5] O. D. Herrera,[2] D. Hewett†,[2] R. Hibbard,[2] D. G. Hicks,[2,28] D. P. Higginson,[2] D. Hill,[1] K. Hill,[14] T. Hilsabeck,[2] D. E. Hinkel,[2] D. D. Ho,[2] V. K. Ho,[1] J. K. Hoffer,[5] N. M. Hoffman,[5] M. Hohenberger,[2] M. Hohensee,[2] W. Hoke,[1] D. Holdener,[2] F. Holdener,[2] J. P. Holder,[2] B. Holko,[1] D. Holunga,[2] J. F. Holzrichter,[2] J. Honig,[2] D. Hoover,[1] D. Hopkins,[2] L. F. Berzak Hopkins,[2] M. Hoppe,Jr.,[1] M. L. Hoppe,Sr.,[1] J. Horner,[2] R. Hornung,[2] C. J. Horsfield,[23] J. Horvath,[2] D. Hotaling,[2] R. House,[2] L. Howell,[2] W. W. Hsing,[2] S. X. Hu,[10] H. Huang,[1] J. Huckins,[2] H. Hui,[2] K. D. Humbird,[2] J. Hund,[1] J. Hunt,[2] O. A. Hurricane,[2] M. Hutton,[2] K. H.-K. Huynh,[2] L. Inandan,[1] C. Iglesias,[2] I. V. Igumenshchev,[10] I. Ivanovich,[29] N. Izumi,[2] M. Jackson,[1] J. Jackson,[2] S. D. Jacobs†,[10] G. James,[2] K. Jancaitis,[2] J. Jarboe,[2] L. C. Jarrott,[2] D. Jasion,[1] J. Jaquez,[1] J. Jeet,[2] A. E. Jenei,[2] J. Jensen,[1] J. Jimenez,[2] R. Jimenez,[1] D. Jobe,[16] Z. Johal,[1] H. M. Johns,[5] D. Johnson,[7] M. A. Johnson,[2] M. Gatu Johnson,[3] R. J. Johnson,[2] S. Johnson,[2] S. A. Johnson,[2] T. Johnson,[3] K. Jones,[7] O. Jones†,[2] M. Jones,[7] R. Jorge,[1] H. J. Jorgenson,[5] M. Julian,[1] B.I. Jun,[2] R. Jungquist,[10] J. Kaae,[1] N. Kabadi,[3] D. Kaczala,[1] D. Kalantar,[2] K. Kangas,[1] V. V. Karasiev,[10] M. Karasik,[30] V. Karpenko,[2] A. Kasarky,[16] K. Kasper,[2] R. Kauffman,[2] M. I. Kaufman,[6] C. Keane,[2,31] L. Keaty,[1] L. Kegelmeyer,[2] P. A. Keiter,[5] P. A. Kellett,[21] J. Kellogg,[7] J. H. Kelly,[10] S. Kemic,[5] A. J. Kemp,[2] G. E. Kemp,[2] G. D. Kerbel,[2] D. Kershaw,[2] S. M. Kerr,[2] T. J. Kessler,[10] M. H. Key,[2] S. F. Khan,[2] H. Khater,[2] C. Kiikka,[2] J. Kilkenny,[1] Y. Kim,[5] Y.-J. Kim,[2] J. Kimko,[2] M. Kimmel,[7] J. M. Kindel,[16] J. King,[2] R. K. Kirkwood,[2] L. Klaus,[2] D. Klem,[2] J. L. Kline,[5] J. Klingmann,[2] G. Kluth,[15] P. Knapp,[7] J. Knauer,[10] J. Knipping,[1] M. Knudson,[7] D. Kobs,[1] J. Koch†,[2] T. Kohut,[2] C. Kong,[1] J. M. Koning,[2] P. Koning,[2] S. Konior,[1] H. Kornblum,[2] L. B. Kot,[5] B. Kozioziemski,[2] M. Kozlowski,[2] P. M. Kozlowski,[5] J. Krammen,[2] N. S. Krasheninnikova,[5] C. M. Krauland,[1] B. Kraus,[14] W. Krauser,[5] J. D. Kress,[5] A. L. Kritcher,[2] E. Krieger,[2] J. J. Kroll,[2] W. L. Kruer,[2] M. K. G. Kruse,[2] S. Kucheyev,[2] M. Kumbera,[2] S. Kumpan,[2] J. Kunimune,[3] E. Kur,[2] B. Kustowski,[2] T. J. T. Kwan,[5] G. A. Kyrala,[5] S. Laffite,[15] M. Lafon,[15] K. LaFortune,[18] B. Lahmann,[3,2] B. Lairson,[9] O. L. Landen,[2] J. Langenbrunner,[5] L. Lagin,[2] T. Land,[2] M. Lane,[2] D. Laney,[2] A. B. Langdon,[2] S. H. Langer,[2] A. Langro,[2] N. E. Lanier,[5] T. E. Lanier,[2] D. Larson,[2] B. F. Lasinski,[2] D. Lassle,[2] D. LaTray,[2] G. Lau,[2] N. Lau,[1] C. Laumann,[2] A. Laurence,[1] T. A. Laurence,[2] J. Lawson,[6] H. P. Le,[2] R. R. Leach,[2] L. Leal,[1] A. Leatherland,[23] K. LeChien,[2] B. Lechleiter,[2] A. Lee,[2] M. Lee,[1] T. Lee,[1] R. J. Leeper,[5] E. Lefebvre,[15] J.-P. Leidinger,[15] B. LeMire,[2] R. W. Lemke,[7] N. C. Lemos,[2] S. Le Pape,[2,32] R. Lerche,[2] S. Lerner,[2] S. Letts,[2] K. Levedahl,[16] T. Lewis,[2] C. K. Li,[3] H. Li,[2] J. Li,[2] W. Liao,[2] Z. M. Liao,[2] D. Liedahl,[2] J. Liebman,[2] G. Lindford,[2] E. L. Lindman,[5] J. D. Lindl,[2] H. Loey,[2] R. A. London,[2] F. Long,[7] E. N. Loomis,[5] F. E. Lopez,[5] H. Lopez,[9] E. Losbanos,[1] S. Loucks,[10] R. Lowe-Webb,[2] E. Lundgren,[1] A. P. Ludwigsen,[2] R. Luo,[1] J. Lusk,[2] R. Lyons,[2] T. Ma,[2] Y. Macallop,[13] M. J. MacDonald,[2] B. J. MacGowan,[2] J. M. Mack,[5] A. J. Mackinnon,[2] S. A. MacLaren,[2] A. G. MacPhee,[2] G. R. Magelssen,[5] J. Magoon,[10] R. M. Malone,[6] T. Malsbury,[2] R. Managan,[2] R. Mancini,[33] K. Manes,[2] D. Maney†,[2] D. Manha,[2] O. M. Mannion,[7] A. M. Manuel,[2] M. J.-E. Manuel,[1] E. Mapoles,[2] G. Mara,[2] T. Marcotte,[1] E. Marin,[1] M. M. Marinak,[2] D. A. Mariscal,[2] E. F. Mariscal,[2] E. V. Marley,[2] J. A. Marozas,[10] R. Marquez,[1] C. D. Marshall,[2] F. J. Marshall,[10] M. Marshall,[10] S. Marshall,[16] J. Marticorena,[2] J. I. Martinez,[5] D. Martinez,[2] I. Maslennikov,[2] D. Mason,[2] R. J. Mason,[5] L. Masse,[2,15] W. Massey,[2] P.-E. Masson-Laborde,[15,34] N. D. Masters,[2] D. Mathisen,[2] E. Mathison,[1] J. Matone,[2] M. J. Matthews,[2] C. Mattoon,[2] T. R. Mattsson,[7] K. Matzen,[7] C. W. Mauche,[2] M. Mauldin,[1] T. McAbee,[2] M. McBurney,[2] T. Mccarville,[2] R. L. McCrory,Jr.,[10] A. M. McEvoy,[5] C. McGuffey,[1] M. Mcinnis,[1] P. McKenty,[10] M. S. McKinley,[2] J. B. McLeod,[2] A. McPherson,[7] B. Mcquillan†,[1] M. Meamber,[2] K. D. Meaney,[5] N. B. Meezan,[2] R. Meissner,[2] T. A. Mehlhorn,[7] N. C. Mehta,[2] J. Menapace,[2] F. E. Merrill,[5] B. T. Merritt,[2] E. C. Merritt,[5] D. D. Meyerhofer,[5] S. Mezyk,[2] R. J. Mich,[2] P. A. Michel,[2] D. Milam,[2] C. Miller,[2] D. Miller,[2] D. S. Miller,[2] E. Miller,[2] E. K. Miller,[6] J. Miller†,[2] M. Miller,[2] P. E. Miller,[2] T. Miller,[1] W.

Miller,[1] V. Miller-Kamm,[2] M. Millot,[2] J. L. Milovich,[2] P. Minner,[2] J.-L. Miquel,[15] S. Mitchell,[2] K. Molvig,[5] R. C. Montesanti,[2] D. S. Montgomery,[5] M. Monticelli,[2] A. Montoya,[7] J. D. Moody,[2] A. S. Moore,[2] E. Moore,[2] M. Moran,[2] J. C. Moreno,[2] K. Moreno,[1] B. E. Morgan,[2] T. Morrow,[5] J. W. Morton,[23] E. Moses,[2] K. Moy,[6] R. Muir,[2] M. S. Murillo,[35, 36] J. E. Murray,[2] J. R. Murray[†,2] D. H. Munro,[2] T. J. Murphy,[5] F. M. Munteanu,[2] J. Nafziger,[1] T. Nagayama,[7] S. R. Nagel,[2] R. Nast,[1] R. A. Negres,[2] A. Nelson,[7] D. Nelson,[10] J. Nelson,[2] S. Nelson,[16] S. Nemethy,[2] P. Neumayer,[2, 37] K. Newman,[2] M. Newton,[2] H. Nguyen,[2] J.-M. G. Di Nicola,[2] P. Di Nicola,[2] C. Niemann,[2, 38] A. Nikroo,[2] P. M. Nilson,[10] A. Nobile,[5] V. Noorai,[1] R. C. Nora,[2] M. Norton,[2] M. Nostrand,[2] V. Note,[2] S. Novell,[2] P. F. Nowak,[2] A. Nunez,[1] R. A. Nyholm,[2] M. O'Brien,[2] A. Oceguera,[2] J. A. Oertel,[5] A. L. Oesterle,[39] J. Okui,[2] B. Olejniczak,[2] J. Oliveira,[2] P. Olsen,[2] B. Olson,[2] K. Olson,[2] R. E. Olson,[5] Y. P. Opachich,[2] N. Orsi,[2] C. D. Orth,[2] M. Owen,[2] S. Padalino,[2, 40] E. Padilla,[2] R. Paguio,[1] S. Paguio,[1] J. Paisner,[5] S. Pajoom,[1] A. Pak,[2] S. Palaniyappan,[5] K. Palma,[2] T. Pannell,[2] F. Papp,[2] D. Paras,[1] T. Parham,[2] H.-S. Park,[2] A. Pasternak,[13] S. Patankar,[2] M. V. Patel,[2] P. K. Patel,[17] R. Patterson,[2] S. Patterson,[2] B. Paul,[9] M. Paul,[2] E. Pauli,[2] O. T. Pearce,[2] J. Pearcy,[3] A. Pedretti,[2] B. Pedrotti,[2] A. Peer,[2] L. J. Pelz,[2] B. Penetrante[†,2] J. Penner,[2] A. Perez,[1] L. J. Perkins,[2] E. Pernice,[2] T. S. Perry,[5] S. Person,[2] D. Petersen,[2] T. Petersen,[2] D. L. Peterson[†,5] E. B. Peterson,[1] J. E. Peterson,[2] J. L. Peterson,[2] K. Peterson,[7] R. R. Peterson,[5] R. D. Petrasso,[3] F. Philippe,[15] D. Phillion,[2] T. J. Phipps,[1] E. Piceno,[1] L. Pickworth,[41] Y. Ping,[2] J. Pino,[2] K. Piston,[2] R. Plummer,[2] G. D. Pollack,[5] S. M. Pollaine,[2] B. B. Pollock,[2] D. Ponce,[1] J. Ponce,[1] J. Pontelandolfo,[1] J. L. Porter,[7] J. Post,[2] O. Poujade,[15, 34] C. Powell,[2] H. Powell[†,2] G. Power,[2] M. Pozulp,[2] M. Prantil,[2] M. Prasad,[2] S. Pratuch,[2] S. Price,[1] K. Primdahl,[2] S. Prisbrey,[2] R. Procassini,[2] A. Pruyne,[10] B. Pudliner,[2] S. R. Qiu,[2] K. Quan,[1] M. Quinn,[1] J. Quintenz,[1] P. B. Radha,[10] F. Rainer,[2] J. E. Ralph,[2] K. S. Raman,[2] R. Raman,[2] P. W. Rambo,[2] S. Rana,[2] A. Randewich,[23] D. Rardin,[2] M. Ratledge,[1] N. Ravelo,[1] F. Ravizza,[2] M. Rayce,[2] A. Raymond,[1] B. Raymond,[2] B. Reed,[2] C. Reed,[1] S. Regan,[10] B . Reichelt,[3] V. Reis,[16] S. Reisdorf,[2] V. Rekow,[2] B. A. Remington,[2] A. Rendon,[2] W. Requieron,[1] M. Rever,[2] H. Reynolds,[1] J. Reynolds,[1] J. Rhodes,[2] M. Rhodes,[2] M. C. Richardson,[10, 42] B. Rice,[10] N. G. Rice,[1] R. Rieben,[2] A. Rigatti,[10] S. Riggs,[2] H. G. Rinderknecht,[10] K. Ring,[1] B. Riordan,[1] R. Riquier,[15] C. Rivers,[1] D. Roberts,[2] V. Roberts,[2] G. Robertson,[7] H. F. Robey,[5] J. Robles,[1] P. Rocha,[2] G. Rochau,[7] J. Rodriguez,[1] S. Rodriguez,[2] M. D. Rosen,[2] M. Rosenberg,[10] G. Ross,[2] J. S. Ross,[2] P. Ross,[16] J. Rouse,[2] D. Rovang,[7] A. M. Rubenchik[†,2] M. S. Rubery,[2] C. L. Ruiz,[7] M. Rushford,[2] B. Russ,[1] J. R. Rygg,[10] B. S. Ryujin,[2] R. A. Sacks,[2] R. F. Sacks,[5] K. Saito,[1] T. Salmon,[2] J. D. Salmonson,[2] J. Sanchez,[2] S. Samuelson,[16] M. Sanchez,[7] C. Sangster,[10] A. Saroyan,[2] J. Sater,[2] A. Satsangi,[16] S. Sauers,[2] R. Saunders,[2] J. P. Sauppe,[5] R. Sawicki,[2] D. Sayre,[2] M. Scanlan,[2] K. Schaffers,[2] G. T. Schappert,[5] S. Schiaffino[†,2] D. J. Schlossberg,[2] D. W. Schmidt,[5] J. M. Smidt,[5] D. H. G. Schneider,[2] M. B. Schneider,[2] R. Schneider,[16] M. Schoff,[1] M. Schollmeier,[7] C. R. Schroeder,[2] S. E. Schrauth,[2] H. A. Scott,[2] I. Scott,[1] J. M. Scott,[5] R. H. H. Scott,[43] C. R. Scullard,[2] T. Sedillo,[5] F. H. Seguin,[3] W. Seka,[10] J. Senecal,[2] S. M. Sepke,[2] L. Seppala,[2] K. Sequoia,[1] J. Severyn,[2] J. M. Sevier,[2] N. Sewell,[2] S. Seznec,[15] R. C. Shah,[10] J. Shamlian,[10] D. Shaughnessy,[2] M. Shaw,[2] R. Shaw,[2] C. Shearer,[1] R. Shelton,[2] N. Shen,[2] M. W. Sherlock,[2] A. I. Shestakov,[2] E. L. Shi,[2] S. J. Shin,[2] N. Shingleton,[2] W. Shmayda,[10] M Shor,[2] M. Shoup,[10] C. Shuldberg,[1] L. Siegel,[2] F. J. Silva,[1] A. N. Simakov,[5] B. T. Sims,[16] D. Sinars,[7] P. Singh,[1] H. Sio,[3, 2] K. Skulina,[2] S. Skupsky,[10] S. Slutz,[7] M. Sluyter[†,16] V. A. Smalyuk,[2] D. Smauley,[2] R. M. Smeltser,[7] C. Smith,[2] I. Smith,[7] J. Smith,[1] L. Smith,[2] R. Smith,[2] R. Smith,[9] M. Schölmerich,[2] R. Sohn,[1] S. Sommer,[2] C. Sorce,[10] M. Sorem,[5] J. M. Soures,[10] M. L. Spaeth,[2] B. K. Spears,[2] S. Speas,[7] D. Speck,[2] R. Speck,[2] J. Spears,[2] T. Spinka,[2] P. T. Springer,[2] M. Stadermann,[2] B. Stahl,[1] J. Stahoviak,[7] J. Stanley,[2] L. G. Stanton,[2, 44] R. Steele,[2] W. Steele[†,2] D. Steinman[†,1] R. Stemke,[1] R. Stephens,[1] S. Sterbenz,[6] P. Sterne,[2] D. Stevens,[2] J. Stevers,[2] C. B. Still[†,2] C. Stoeckl,[10] W. Stoeffl,[2] J. S. Stolken,[2] C. Stolz,[2] E. Storm,[2] G. Stone,[2] S. Stoupin,[2] E. Stout,[2] I. Stowers,[2] R. Strauser,[1] H. Streckart,[1] J. Streit,[13] D. J. Strozzi,[2] J. Stutz,[1] L. Summers,[2] T. Suratwala,[2] G. Sutcliffe,[3] L. J. Suter,[2] S. B. Sutton,[2] V. Svidzinski,[2] G. Swadling,[2] W. Sweet,[1] A. Szoke[†,2] M. Tabak,[2] M. Takagi,[2] A. Tambazidis,[1] V. Tang,[2] M. Taranowski,[2] L. A. Taylor,[2] S. Telford,[2] W. Theobald,[10] M. Thi,[1] A. Thomas,[2] C. A. Thomas,[2, 10] I. Thomas[†,2] R. Thomas[†,7] I. J. Thompson,[2] A. Thongstisubskul,[1] C. B. Thorsness,[2] G. Tietbohl,[2] R. E. Tipton,[2] M. Tobin,[2] N. Tomlin,[1] R. Tommasini,[2] A. J. Toreja,[2] J. Torres,[7] R. P. J. Town,[2] S. Townsend,[2] J. Trenholme[†,2] A. Trivelpiece,[2] C. Trosseille,[2] H. Truax,[1] D. Trummer,[2] S. Trummer,[2] T. Truong,[16] D. Tubbs,[5] E. R. Tubman,[2] T. Tunnell,[6] D. Turnbull,[10] R. E. Turner,[2] M. Ulitsky,[2] R. Upadhye,[2] J. L. Vaher,[2] P. VanArsdall,[2] D. VanBlarcom,[2] M. Vandenboomgaerde,[15] R. VanQuinlan,[2] B. M. Van Wonterghem,[2] W. S. Varnum,[5] A. L. Velikovich,[30] A. Vella,[2] C. P. Verdon,[16] B. Vermillion,[1] S. Vernon,[2] R. Vesey,[7] J. Vickers,[1] R. M. Vignes,[2] M. Visosky,[16] J. Vocke,[1] P. L. Volegov,[5] S. Vonhof,[1] R. Von Rotz,[2] H. X. Vu,[5] M. Vu,[1] D. Wall,[1] J. Wall,[1] R. Wallace,[2] B. Wallin,[2] D. Walmer,[2] C. A. Walsh,[2] C. F. Walters,[2] C. Waltz,[2] A. Wan,[2] A. Wang,[2] Y. Wang,[2] J. S. Wark,[24] B. E. Warner,[2] J. Watson,[2] R. G. Watt,[5] P. Watts,[2] J. Weaver,[30] R. P. Weaver,[5] S. Weaver,[2] C. R. Weber,[2] P. Weber,[2] S. V. Weber,[2] P.

Wegner,[2] B. Welday,[2] L. Welser-Sherrill,[5] K. Weiss,[2] K. Widmann,[2] G. F. Wheeler,[2] W. Whistler†,[2] R. K. White,[2] H. D. Whitley,[2] P. Whitman,[2] M. E. Wickett,[2] C. Widmayer,[2] J. Wiedwald,[2] R. Wilcox,[12] S. Wilcox,[2] C. Wild,[22] B. H. Wilde,[5] C. H. Wilde,[5] K. Wilhelmsen,[2] M. D. Wilke†,[5] H. Wilkens,[1] P. Wilkins,[2] S. C. Wilks,[2] E. A. Williams,[2] G. J. Williams,[2] W. Williams,[2] W. H. Williams,[2] D. C. Wilson,[5] B. Wilson,[2] E. Wilson,[2] R. Wilson,[2] S. Winters,[2] P. J. Wisoff,[2] M. Wittman,[10] J. Wolfe,[2] A. Wong,[2] K. W. Wong,[2] L. Wong,[2] N. Wong,[2] R. Wood,[2] D. Woodhouse,[1] J. Woodruff†,[2] D. T. Woods,[2] S. Woods,[1] B. N. Woodworth,[2] E. Wooten,[1] A. Wootton,[2] K. Work,[6] J. B. Workman,[5] J. Wright,[2] M. Wu,[7] C. Wuest,[6] F. J. Wysocki,[5] H. Xu,[1] M. Yamaguchi,[1] B. Yang,[2] S. T. Yang,[2] J. Yatabe,[2] C. B.Yeamans,[2] B. C. Yee,[2] S.A. Yi,[5] L. Yin,[5] B. Young,[2] C. S. Young,[5] C. V. Young,[2] P. Young,[2] K. Youngblood,[1] J. Yu,[2] R. Zacharias,[2] G. Zagaris,[2] N. Zaitseva,[2] F. Zaka,[2] F. Ze,[2] B. Zeiger,[9] M. Zika,[2] G. B. Zimmerman,[2] T. Zobrist,[2] J. D. Zuegel,[10] A. B. Zylstra,[2] and (The Indirect Drive ICF Collaboration)

[1] *General Atomics, San Diego, California 92186, USA*
[2] *Lawrence Livermore National Laboratory, P.O. Box 808, Livermore, California 94551-0808, USA*
[3] *Massachusetts Institute of Technology, Cambridge, Massachusetts 02139, USA*
[4] *Polymath Research Inc., 827 Bonde Ct., Pleasanton, CA 94566*
[5] *Los Alamos National Laboratory, Mail Stop F663, Los Alamos, New Mexico 87545, USA*
[6] *Nevada National Security Site, 232 Energy Way, North Las Vegas, NV, 89030, USA*
[7] *Sandia National Laboratories, P.O. Box 5800 Albuquerque, New Mexico 87123, USA*
[8] *Imperial College London, Plasma Physics, South Kensington Campus, London, SW7 2AZ, UK*
[9] *Luxel Corporation, P.O. Box 1879, 60 Saltspring Dr., Friday Harbor, WA 98250, USA*
[10] *Laboratory for Laser Energetics, University of Rochester, Rochester, New York 14623, USA*
[11] *University of California at Berkeley, Dept. of Nuclear Engineering,*
4165 Etcheverry Hall, Berkeley, CA 94720-1730, USA
[12] *Lawrence Berkeley National Laboratory, 1 Cyclotron Road, Berkeley, CA 94720, USA*
[13] *Gryphon Technologies, 303 Lindbergh Ave., Livermore, CA 94551, USA*
[14] *Princeton Plasma Physics Laboratory, 100 Stellarator Road, Princeton, NJ 08540, USA*
[15] *CEA/DAM/DIF, 91297 Arpajon cedex, France*
[16] *National Nuclear Security Administration, Office of Defense Programs,*
United States Department of Energy, Washington, DC 20585, USA
[17] *Focused Energy Inc., 11525-B Stonehollow Dr. Suite 200, Austin, TX 78758, USA*
[18] *SLAC National Accelerator Laboratory, Menlo Park, California 94025, USA*
[19] *University of New Mexico, Dept. of Nuclear Engineering,*
MSC01 1120, 1 University of New Mexico, Albuquerque, NM 87131-0001
[20] *University of Michigan, Climate & Space Research Building,*
2455 Hayward Street Ann Arbor, MI 48109-2143, USA
[21] *Kentech Instruments Ltd., Isis Building, Howbery Park, Wallingford, Oxfordshire, OX10 8BD, UK*
[22] *Diamond Materials Gmbh, 79108 Freiburg, Germany*
[23] *Atomic Weapons Establishment, Aldermaston, RG7 4PR, United Kingdom*
[24] *Department of Physics, Clarendon Lab, University of Oxford, Parks Road, Oxford, OX1 3PU, UK*
[25] *Spectral Sciences Inc., 4 Fourth Ave, Burlington, MA 01803-3304, USA*
[26] *Fraunhofer Institute for Laser Technology ILT, 52066 Aachen, Germany*
[27] *RWTH Aachen University, 52066 Aachen, Germany*
[28] *Optical Sciences Centre, Department of Physics and Astronomy,*
Swinburne University of Technology, Hawthorn, Victoria 3122, AU
[29] *University of Michigan, 500 S State St, Ann Arbor, MI 48109*
[30] *United States Naval Research Laboratory, Plasma Physics Division,*
4555 Overlook Ave SW, Washington, DC 20375, USA
[31] *Washington State University, Office of Research,*
P.O. Box 641060, Pullman, WA 99164-1060, USA
[32] *Laboratoire pour l'utilisation des Lasers Intenses chez École Polytechnique, F-91128 Palaiseau cedex, France*
[33] *University of Nevada at Reno, Dept. of Physics,*
MS 0220, 1664 N. Virginia St., Reno, NV 89557, USA
[34] *Université of Paris-Saclay, CEA, LMCE, 91680 Bruyères-le-Châtel, France*
[35] *Department of Computational Mathematics, Science and Engineering,*
Michigan State University, East Lansing, Michigan 48824, USA
[36] *Department of Computational Mathematics, Science and Engineering,*
Michigan State University, East Lansing, Michigan 48824
[37] *GSI Helmholtzzentrum für Schwerionenforschung GmbH, Planckstrasse 1, 64291 Darmstadt, Germany*
[38] *University of California at Los Angeles, Dept. of Physics & Astronomy,*
475 Portola Plaza, Los Angeles, CA 90095-1547, USA
[39] *Sutter Instrument, 1 Digital Dr., Novator, CA 94949*
[40] *SUNY Geneseo, Dept. of Physics & Astronomy,*
Integrated Science Center, Geneseo, NY 14454, USA

[41] *Lund University, MAX IV Laboratory, Box 118, 221 00 Lund, Sweden*
[42] *Townes Laser Institute, University of Central Florida, Orlando, FL 32816, USA*
[43] *Central Laser Facility, STFC Rutherford Appleton Laboratory, Harwell Oxford, OC11 0QX, UK*
[44] *Dept. of Mathematics and Statistics, San Jose State University, San Jose, California 95192, USA*
(Dated: January 2, 2024)

On December 5, 2022 an indirect drive fusion implosion on the National Ignition Facility (NIF) achieved a target gain, G_{target}, of 1.5. This is the first laboratory demonstration of exceeding "scientific breakeven" (or $G_{target} > 1$) where 2.05 MJ of 351 nm laser light produced 3.1 MJ of total fusion yield, a result which significantly exceeds the Lawson criterion for fusion ignition as reported in a previous NIF implosion [Abu-Shawareb, *et al* (Indirect Drive ICF Collaboration), Phys. Rev. Lett. **129** 075001 (2022)]. This achievement is the culmination of more than 5 decades of research and gives proof that laboratory fusion, based on fundamental physics principles, is possible. This letter reports on the target, laser, design and experimental advancements that led to this result.

The quest for laboratory fusion and the possibility of a nearly limitless source of low-carbon and low-radiation energy likely began in the 1920s shortly after Harkins, Perrin and Eddington conjectured self-sustaining hydrogen fusion as the primary system fueling the sun [1–3]. This idea was inspired by Aston's discovery [4], using his newly invented mass spectrograph, that four hydrogen atoms are heavier than one helium atom. In 1928 Gamow [5] developed the mathematical basis for quantum tunneling which allowed Atkinson and Houtermans [6] to make the first estimates of the stellar fusion rate, supporting the conjecture of self-sustaining fusion powering the stars. The first example of human-caused fusion was made by Oliphant [7] in 1933 and in 1939 Bethe [8] developed the stellar nucleosynthesis theory of hydrogen fusion powering the sun. In 1946 Thomson and Blackman [British patent 817681] proposed a fusion reactor using a "Z-pinch" concept and in 1957 Lawson[9] published his famous minimum product of density n_e and energy confinement time, τ_e, required for self-sustaining nuclear fusion ignition. The most ubiquitous example of self-sustaining nuclear fusion in the universe is stars and the closest example is our sun where gravitational forces provide the natural confinement, compression and heating required for fusion. On Earth, these conditions occur in a thermonuclear weapon. A fundamental obstacle to realizing a fusion energy source has been the ability to control and heat a plasma to the conditions required for ignition and to confine the plasma at these conditions over long enough time scales such that more fusion energy is produced than was supplied to initiate the reaction.

Over the approximately hundred years since fusion was discovered, significant research has been directed to develop multiple nuclear fusion concepts. These concepts broadly fall into two categories depending on the method to confine the plasma. One method uses magnetic fields and employs devices such as tokamaks, stellarators and magnetic pinches [10]. The second method temporarily confines the fusing plasma with the inertia of a surrounding material and is therefore called inertial confinement, the approach used in our experiment. Following the in-

vention of the laser in 1960, several authors proposed using lasers to trigger nuclear fusion reactions [11–13]. Nuckolls proposed an Inertial Confinement Fusion (ICF) scheme that utilized the radiative power of intense lasers to compress, heat and confine a reacting plasma [14]. ICF schemes have since been extended to indirect drive [15] while laser direct drive [16] and magnetic drive [17] are also being pursued.
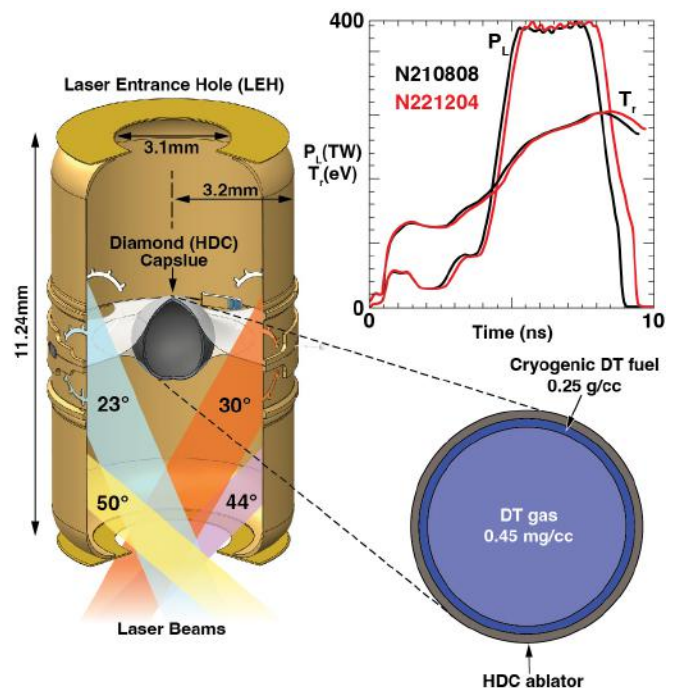

FIG. 1. Left: Schematic of the target and laser configuration including the hohlraum. Bottom-right: The HDC capsule and DT fuel configuration. Top-right: total laser power vs. time and radiation temperature, T_r, as a function of time. The high-density-carbon (HDC) capsule thickness was increased by $\sim$ 7% and the laser energy was increased by $\sim$ 7.9% for N221204 (red line) compared to N210808 (black line).

An indirect drive implosion at the National Ignition Facility [18–21] occurs by directing 1 to 2 MJ of 351 nm laser energy to the inside surface of a high-Z element

cylindrical enclosure, a hohlraum (see Fig. 1), which converts the laser energy to x-rays with a nearly Planckian energy distribution and a peak temperature of about 300 eV. The x-rays ablate the outside of a ~ 2 mm diameter high density carbon (HDC) capsule with a frozen layer of deuterium-tritium (DT) fuel coated on the inside and DT vapor in thermodynamic equilibrium inside the fuel shell. Most laboratory nuclear fusion approaches use a 50-50 mixture of DT fuel based on its high reactivity rate for a given temperature. DT fusion produces 14.1 MeV neutrons and 3.5 MeV alpha particles. Alpha heating and pdV (DT plasma pressure $\times$ volumetric change) compressional work is balanced by bremsstrahlung x-ray emission and thermal conduction losses leading to a minimum plasma temperature of $T \approx T_e \approx T_i = 4.3$ keV for self-heating fusion in a clean implosion where there are no additional sources of power degradation. Ablation from the x-ray drive accelerates the remaining ablator shell inward reaching a speed of 380 to 400 km/s, compressing the cold DT fuel 1000 to 2000$\times$ in density and heating the inside vapor to 4-6 keV at minimum volume, a stage of the implosion called "stagnation." If the central hot spot ignites and if the heating rate from fusion alphas exceeds the other losses in the system then fusion burn will rapidly expand into the surrounding cold fuel. Following ignition the DT temperature increases to well over 10 keV.

In August 2021 an indirect drive DT implosion experiment at the National Ignition Facility (NIF) at Lawrence Livermore National Laboratory in Livermore, CA achieved a target gain of 0.72 (ratio of total yield energy to total laser energy delivered to the target) and exceeded the Lawson ignition criterion [22–24]. Simulations and analytic theory showed that further increases in the target gain required increases in total areal density (ρR, the average integral of the mass density over a radial chord) and energy coupled to the fuel, beyond what had been obtained with the current target design [15]. Our hypothesis was that the fuel burn-up fraction (defined as the fraction of DT fuel that has undergone fusion) and the resulting yield could be improved by increasing the coupled energy and consequently the implosion kinetic energy; however, there was also significant risk that ablator-fuel mix could preheat much of the fuel [25] limiting the yield increase. Such an implosion was subsequently performed on NIF in December 2022 and achieved the highest ever target gain of 1.5, exceeding scientific breakeven and the National Academy of Sciences definition of the ignition threshold [26]. In this article and companion papers [27–29], we describe the design, theory, experimental parameters, and observables of the first laboratory scale system that used indirect drive to exceed scientific breakeven where the pressure and confinement time required to produce more fusion energy than supplied to the target, or $G_{target} > 1$, was achieved.

Figure 2 shows a three order of magnitude improvement in target gain over 11 years of experiments starting with the 2011 implosions that first used 50/50 DT
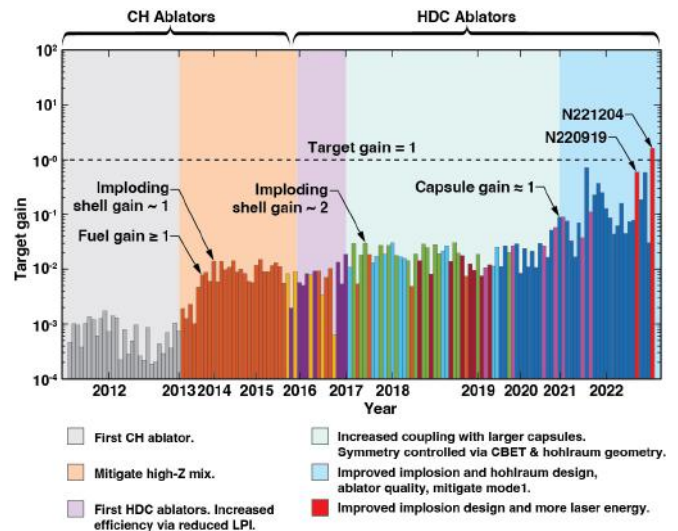
FIG. 2. Target gain vs. calendar date. The horizontal labels mark the beginning of each year. The color of the narrow target gain bars represents different implosion designs and the dashed horizontal line represents the target gain = 1 per the NAS ignition criteria [26].

fuel in a CH (plastic) ablator [30–32]. These advances were enabled using experiments focused on subsets of the complete system [33] and integrated experiments on cryogenically-layered targets [34] as well as theory and detailed radiation hydrodynamic modeling to continuously improve the implosion quality. While more details can be found in Ref. [22], Appendix A summarizes the key steps from 2011 to exceeding Lawson's criterion in a 2021 experiment.

Following the August 2021 result, a series of five similar implosions, with the currently achievable small range of uncontrolled shot-to-shot variations in laser delivery and target quality, showed that residual low mode drive asymmetries and mix could still degrade the performance by factors ranging from ~ 2 to ~ 5, respectively [35]. Asymmetry in the compression primarily arises from variations in laser delivery and the capsule wall thickness uniformity [36, 37] while mix primarily arises from hydrodynamic instability growth, seeded by capsule defects, such as surface pits and debris as well as from the perturbation induced by the capsule fill tube [38–40]. Details of the relative capsule quality are given in the appendix of the companion experimental paper [41]. These degradations were identified as the primary cause of the observed shot-to-shot variability in fusion yield that results from proximity to the ignition threshold [42]. Together, implosion asymmetry and hotspot mixing push the threshold for ignition and high fuel gain to higher implosion kinetic energy [28]. Radiation hydrodynamic computer models Lasnex [43] and HYDRA [44], which employ highly detailed physics descriptions of laser transport, radiation transfer, hydrodynamics, thermodynamics, and nuclear reaction processes [45–47], backed by theory, showed that

a modest increase in laser energy driving a thicker capsule could decrease the sensitivity to low mode and mix degradations and increase the confinement time and fusion yield [27]. Initiated over six years ago, a focused laser effort [48, 49] based on earlier single quad tests [50] (a quad is a group of four beams in a 2×2 configuration) is described in Appendix B and allowed the NIF laser energy to be increased from 1.9 to 2.05 MJ by September 2022.

The indirect drive target and laser configuration for experiment N221204 (NIF shot notation being NYYM-MDD where N = NIF, YY = year, MM = month, DD = day when the shot countdown began) that is the focus of this letter, is compared with NIF shot N210808 in Fig. 1. In both cases, the lasers are directed onto the inside of a 6.4 mm diameter and 11.24 mm tall gold-lined depleted uranium (DU) hohlraum in four laser cones defined by their angle of incidence (Inner beams: 23 and 30-deg and Outer beams: 44 and 50-deg, with angle specified relative to the vertical axis). The hohlraum is filled with 0.3 mg/cc of pure He gas. The gold lining on the inside surface of the uranium creates a lower x-ray drive spectrum above 1.8 keV photon energy (as compared to pure DU) and prevents DU oxidation. The time dependent laser power and relative power balance between the laser cones are used to control the compression and symmetry of the implosion, respectively. The 2.1 mm diameter HDC ablator capsule containing the DT fuel is suspended in the center of the hohlraum between two 45 nm thickness tent Formvar membranes [51]. The capsule is nanocrystalline HDC of mass 4.25mg. Inside the capsule is a 64.5μm thick layer of solid cryogenic DT fuel of mass of 220μg. The HDC capsule for N221204 uses the same inner radius of 1.05 mm as N210808 but with a thickness increase of $\sim 7\%$. The capsule typically contains a buried tungsten-doped layer to shield the DT fuel from x-ray drive generated preheat in the DT fuel, assisting with higher compression. For N221204 the doped layer is ~ 0.6 at% tungsten as measured by x-ray fluorescence, is 15 μm thick and is positioned with 63 μm of undoped HDC on the outside and 8 μm of undoped HDC on the inside. The areal density of tungsten in the capsule for N221204 is approximately $1.2\times$ relative to prior experiments. Appendix C provides details of the metrology used to assess the target quality.

The increase in laser energy on NIF shot N221204 was limited to a peak power of 440 TW (due to NIF optics damage concerns); this allowed using a longer-duration laser pulse as can be seen in Fig. 1. A design study performed using HYDRA showed that this longer more energetic pulse driving an $\sim 7\%$ thicker (+6 microns) HDC ablator would increase the total areal density, ρR, at peak compression by 15-20% increasing the DT fuel burn up fraction and improving the implosion robustness to degradations compared to N210808 [27]. An adjustment to the radiation drive symmetry was needed since an extended laser pulse allows more hohlraum wall plasma blow-in which eventually impedes inner-beam laser prop-

agation to the hohlraum wall [52–54]. This was accomplished using Cross-Beam Energy Transfer (CBET) [55] with wavelength detuning between the inner and outer cones; minor adjustments were also made to the detailed time-dependent laser powers on all beams. The first test of this new design was on shot N220919 which gave a 1.2 MJ yield even with an oblate hot spot shape, due in part to restrictions on the amount of wavelength detuning which could be safely implemented in the first test. Benchmarking HYDRA simulations [27] against this result showed that additional optimization of CBET and the laser power pulse shape could achieve a symmetric implosion and increase the yield by $\geq 2.5\times$. This was implemented on the second test of this design, NIF shot N221204, which resulted in 3.1 ± 0.16 MJ of yield and a target gain of 1.5, comparable to the design predictions.

A novel "Cognitive Simulation" (CogSim) model [56] was used to assess the 2.05MJ capsule design, and predicted a 14-fold increase in the probability of achieving ignition compared to N210808, with an average expected yield of around 2.5 MJ. Experiment fielding variations in implosion symmetry and target quality have traditionally made performance predictions challenging, even if they can often be understood through post-shot modeling. The CogSim model has enabled significant progress in this by applying a statistical model for performance variations, which is trained on a suite of previous NIF shots and then applied to a proposed design with high-fidelity simulations and machine learning techniques. This statistical model is used to generate detailed distributions of the expected experimental observables, as well as measures of performance robustness, which can inform pre-shot expectations. The N221204 shot marks the first application of the CogSim approach prior to executing the experiment, and is the first shot for which a significant probability of scientific breakeven was predicted.

Stimulated Brillouin laser backscattering (SBS), which reduces the laser coupling to the hohlraum and is a potential source of laser optics damage [57], is estimated from the NIF full-aperture backscatter (FABS) diagnostic [58] and the laser drive diagnostic [59] to be 42 ± 11 kJ (one-σ). The SBS is observed early in peak power and is mostly on the inner cones. Stimulated Raman scattering (SRS), estimated from FABS, is 6 ± 1 kJ (one-σ) and occurs throughout peak power. The backscatter uncertainty includes both measurement error as well as estimated quad-to-quad variations. The fraction of total laser energy coupled to the hohlraum, due to SBS, for shot N221204 is 98% $\pm$ 0.6%. As shown in Fig. 1, the longer pulse of N221204 reached a 2% higher peak x-ray drive temperature as expected given the increasing hohlraum wall albedo in time [60], and confirming no significant late time backscatter losses. Only fast response diode based measurements are available for characterizing the backscatter on high-yield experiments; streaked spectra are not available.

A suite of x-ray and nuclear instruments [61] diagnose the key properties of the fusing plasma, including

the neutron yield and energy spectrum, spatially varying neutron [62] and x-ray emission profiles and emission weighted temperature. These measurements have been of fundamental importance for understanding and optimizing the experimental response to changes in input laser and target conditions and to the deliberate changes in the implosion design. Additionally, the measurements are used to infer key hot spot quantities such as the pressure, energy, and areal density which are used to evaluate different ignition criteria. These measurements and inferences are listed in Table 1 for N221204 and a selection of companion prior experiments. Both x-ray and nuclear instruments are available on high-yield experiments.

The neutron energy spectrum encodes key information about the neutron yield, emission weighted DT ion temperature, velocity flow and the areal density of the DT plasma and remaining shell [63]. Two types of diagnostics measure the neutron energy spectrum, a Magnetic Recoil Spectrometer (MRS) [64] and a suite of 4-5 neutron time of flight (NToF) spectrometers [65, 66]. About 4% of the neutrons are down scattered to lower energies by the surrounding high density fuel and shell as they escape. The down scattered ratio (DSR), defined as the ratio of the number of neutrons in the energy range of 10-12 MeV to those in the range of 13-15 MeV, is proportional to the ρR of the fusing hot spot and surrounding DT fuel [67]. The MRS and three zirconium nuclear activation foils [68], all of which have been absolutely calibrated, are used to measure the yield of un-scattered neutrons. The total neutron yield is inferred by correcting the unscattered number using the relationship $Y_{n_{\text{total}}} = Y_{n_{13-15\text{MeV}}} e^{(4*\text{DSR})}$ [63, 69, 70], which accounts for DT fusion neutrons scattered out of the 13-15 MeV energy range. The resultant yield is $1.12 \times 10^{18} \pm 0.06 \times 10^{18}$ neutrons. In addition to the yield, temperature, and areal density, two orthogonal neutron imaging diagnostics quantify the spatial distribution of the neutron emission. An independent method of estimating the yield, which is cross-calibrated to previous yields and uses the increase in measured x-ray emission from the ignition-reheated hohlraum, is also consistent with a 3.1 MJ yield [71].

Figure 3 shows the two dimensional (2D) time averaged, spatial distribution of neutron emission from two views and the 3D tomographic reconstruction of the neutron emissivity (total neutrons emitted per unit volume) for three experiments where the neutron yield increased by 20-fold culminating in N221204 with a total fusion energy yield of 3.1 ± 0.16 MJ. Figure 3 and Table 1 show that as the fusion yield increases, the temperature and volume of the reacting plasma increase by factors of 2 and 4, respectively. The changes in temperature and volume are associated with the increased rate of α particle self-heating sustaining and initially increasing the temperature and reactivity as the hot spot expands outward after peak compression [35]. The dominant uncertainty in the fusion yield inference stems from systematic, rather than statistical, uncertainty in the measurement and detection

hardware. As the yield increases, the areal density of the system is emission weighted to larger radii, which is why, for a given design, the areal density decreases as the yield increases.

It is also instructive to check the scaling of the observed burn-up fraction between N210808 and N221204 relative to the simple expression [15] for yield limited by the disassembly/explosion phase. The burn-up fraction ratio in the limit of little DT depletion scales [22] as $\frac{\rho R_1}{\rho R_2} \left(\frac{T_1}{T_2}\right)^{m-0.5}$, where $m = 7(1 - 0.2 \ln \langle T \rangle)/\langle T \rangle^{0.2}$ is a good fit to the DT relative reactivity between 5 and 20 keV [72] with $\langle T \rangle = (T_1 + T_2)/2$ and the subscript 1 refers to N221204 and 2 to N210808. For the observed ρR and T ratio of 1.15 ± 0.03 and 1.35 ± 0.1, the predicted burn-up fraction ratio $= 2 \pm 0.25$ is close to the measured ratio of $4.3\%/1.8\% = 2.3$, suggesting we are indeed close to the regime of all the exploding fuel participating in burn. Here we have used the N220919 ρR to compare to N210808 for similar T and hence explosion speed, and used T_{DD} for T, since it is known to be less sensitive to motional broadening than T_{DT} [73]. Putting in numbers and assuming burn is truncated after a 40% increase in radius, as seen for example on N210808, at an average explosion velocity $= \sqrt{kT/2.5M_p}$, where M_p is the proton mass and 2.5 is the average atomic mass of DT, the expected burn-up fraction $= 1 \times 10^{-5} \rho R T^{n-0.5}$ (where $n = 7/T^{0.2}$) is also a consistent 5% for the observed $\rho R = 0.6$ g/cm^2 and $T \approx 10$ keV.

To further contextualize the energy gain and plasma conditions obtained, it is valuable to use these measurements to evaluate traditional metrics of power balance such as the Lawson parameter. The Lawson Criterion for ignition [9] is a statement indicating the crossing of a tipping-point, namely the threshold where plasma self-heating exceeds cooling processes such that a rapid increase in plasma temperature (T_{th}) and fusion reaction-rate is generated. In Lawson's original work, bremsstrahlung x-rays were the only loss mechanism considered, but for ICF systems, bremsstrahlung, electron heat conduction, and negative pdV work, where p is the time-dependent hot spot pressure and V is volume, on expansion [74–76] all counteract self-heating. While Lawson was not considering implosion fusion systems, his alpha-particle trapping case is appropriate for ICF, with some generalization [77] that respects the impulsive nature of ICF implosions. Both the plasma thermal temperature and product of number density and reaction-time, $n\tau$, must be sufficiently high for net power production. Over the past two decades a number of different formulations of the Lawson Criterion for ICF have been developed that leverage different experimentally measured and/or inferred quantities, excluding or including T [69, 75, 78–83], the latter being more directly related to the Lawson Criterion in common use in magnetic fusion. The fuel energy gain, G_{fuel} (see Appendix A), is most directly related to the Lawson triple product $\sim p\tau T$ [84]. Capsule gain, $G_{\text{cap}} = Y_{\text{tot}}/E_{\text{abs}}$, is
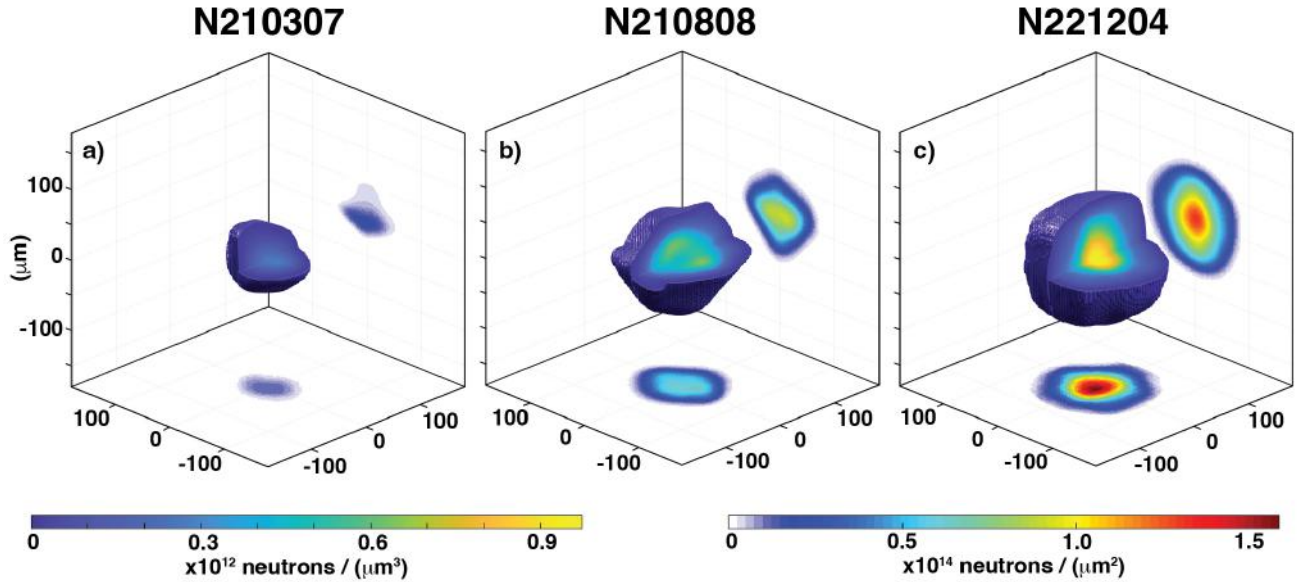
FIG. 3. 3D reconstruction of the time integrated emission-weighted neutron emissivity from two neutron images taken on each shot from orthogonal lines of sight (image projections), for NIF shots: a) N210307, b) N210808 and c) N221204. The left color bar corresponds to the 3D represented volume, the right color bar is for the 2D projections of this volume.

TABLE I. Experimental parameters

NIF shot	N210207	N210307	N210808	N220919	N221204
P_{laser} (TW)	470	487	441	440	440
E_{laser} (MJ)	1.93	1.91	1.89	2.05	2.05
Drive T_{rad} (eV)	304	306	$307^{\text{(a)}}$	313	313
t_{coast} (ns)	1.09	1.26	0.93	0.89	0.78
Y_{total} (MJ)	0.17 ± 0.01	0.14 ± 0.01	1.3 ± 0.07	1.2 ± 0.06	3.1 ± 0.16
T_{DT} (keV)	5.66 ± 0.13	5.55 ± 0.11	10.9 ± 0.4	10.1 ± 0.2	13.1 ± 0.7
T_{DD} (keV)	5.23 ± 0.16	4.87 ± 0.14	8.94 ± 0.4	8.7 ± 0.2	12 ± 1
DSR (%)	3.02 ± 0.16	3.39 ± 0.14	2.72 ± 0.24	3.06 ± 0.14	2.83 ± 0.17
V ($10^5 \mu\text{m}^3$)	3.3 ± 0.3	2.7 ± 0.3	6.4 ± 0.75	6.7 ± 0.9	12.9 ± 1.5
t_{BW} (ps)	137 ± 25	138 ± 20	89 ± 15	92 ± 20	75 ± 15
p_{HS} (Gbar)	304^{+39}_{-30}	323^{+33}_{-28}	561^{+61}_{-53}	518^{+76}_{-62}	608^{+56}_{-59}
E_{HS} (kJ)	$15.1^{+1.9}_{-1.5}$	$13.5^{+1.3}_{-1.1}$	54^{+6}_{-5}	53^{+8}_{-6}	118^{+14}_{-12}
$(\rho R)_{\text{HS}}$ (g/cm^2)	$0.32^{+0.05}_{-0.04}$	$0.35^{+0.04}_{-0.03}$	$0.44^{+0.05}_{-0.04}$	$0.42^{+0.06}_{-0.04}$	$0.44^{+0.06}_{-0.05}$
Burn-up fraction (%)	0.24	0.20	1.77	1.60	4.33
G_{fuel}	$9.8^{+0.6}_{-0.9}$	$8.1^{+0.5}_{-0.7}$	$73.4^{+4.2}_{-6.6}$	$65.8^{+3.8}_{-5.8}$	$172.8^{+10.1}_{-15.3}$
G_{capsule}	0.75 ± 0.05	0.69 ± 0.05	5.8	~ 5	12
G_{target}	0.09	0.07	0.7	0.57	1.5
GLC_H	0.32-0.36	0.18-0.22	2.8	2.5	3.7
$ITFX_\alpha{}^{\text{(b)}}$	1.8 ± 0.2	1.9 ± 0.2	11 ± 2.2	12.6 ± 1.3	28.2 ± 3.7

(a) Indicates average over similar experiments

(b) The experimentally observable ignition threshold factor is $ITFX_\alpha$ [69].

yet another gain definition and compares the total yield to capsule x-ray absorbed energy E_{abs}, whose threshold of unity is at typically 10x higher total yield than G_{fuel}. For indirect-drive, G_{cap} is generally a small fraction of G_{target} while for direct-drive the two terms are synonymous. It is important to note that it is possible to pass any of the alternate versions of Lawson's criterion for ignition without obtaining $G_{\text{target}} > 1$. Indeed, ignition

by these different formulations of Lawson's Criterion was first achieved on NIF experiment N210808 [22] and confirmed by independent analysis [85].

It was shown in [22] that all of the various forms of Lawson's criteria in the context of ICF gave the same qualitative conclusions about the ignition of N210808. So, here we focus on data comparison to just one of the representative criteria, but the one that uniquely includes
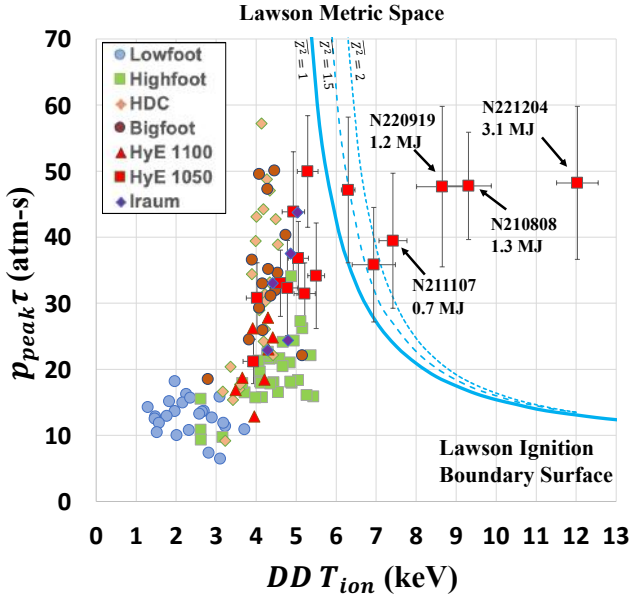
FIG. 4. NIF DT shot data are plotted in the space of inferred hot spot Lawson parameter which corresponds to hot spot peak pressure times burn duration, $p\tau$, and DD ion temperature, which is the temperature T determined by the neutron-time-of-flight spread of 2.5 MeV neutrons that come from deuterium-deuterium fusion. The curves denote the ignition boundary per the GLC equation described in the text assuming no mix (solid) and with a multiplier of 1.5 and 2× on the radiative loss to account for increased levels of higher atomic number mix (dashed curves). Experiments N210808 and N221204 exhibit little mixing, $\overline{Z^2} \sim 1.03 \pm 0.02$, while other experiments can exhibit higher values depending upon capsule quality, fill-tube size, and hydrodynamic instability control. Data from the Hybrid-E series is highlighted as red points, while earlier campaigns are shown in other colors.

the effects of high-Z mixing into the hotspot on the ignition threshold. Framing ignition thermodynamically, as a non-polytropic process where an exponential and irreversible jump in $(pV^\gamma)_{\text{final}} = (pV^\gamma)_{\text{initial}} \exp(GLC_H)$ occurs in the DT hotspot volume due to significant alpha-heating and entropy generation over the moment of implosion stagnation, one finds a condition that is naturally presented in the parameter space of $p\tau$ and T which are familiar to practitioners of magnetic fusion [83]. Namely,

$$\text{GLC}_{\text{H}} = p_{\text{peak}}\tau H(T) \tag{1}$$

with the criterion $\text{GLC}_{\text{H}} > 1$ determining ignition. Here, GLC represents "Generalized Lawson Criterion." $H(T)$ is a complicated function of temperature and a parameter related to bremsstrahlung x-ray enhancement due to high-Z material mixing into the DT hotspot. The peak hotspot pressure, p_{peak}, is inferred using the prescription in [86]. Technically, the confinement timescale, $\tau = \sqrt{T/|\ddot{T}|}$, in Eq. (1) is related to the second time-derivative of hotspot temperature at peak T, which isn't presently measured on the NIF, but under certain as-

sumptions τ can be the same as the measured burn-width. This criterion, intermediate in conservatism as reviewed in the companion articles [28, 29], is over-plotted in Fig. 4, with the dashed curves representing different plausible levels of enhanced radiative loss from high-Z mix into the hot spot consistent with observations [87]. N221204, and other igniting experiments, distinguish themselves in Fig. 4 by increasing T at nearly constant $p_{\text{peak}}\tau$ qualitatively consistent with expectations. Gain values and ignition metrics are shown in Table I for the NIF experiment N210808, the previous record, and N221204.

In summary, the December 5, 2022 experiment on the National Ignition Facility, N221204, was the first time that fusion target gain was unambiguously achieved in the laboratory in any fusion scheme. The demonstrated level of target gain on N221204 of 1.5 times is a proof of principle that controlled laboratory fusion energy is possible. Note that $G_{\text{target}} > 1$ does not imply net energy gain from a practical fusion energy perspective because the energy consumed by the NIF laser facility is typically 100× larger than E_{laser}. The NIF laser architecture and target configuration was chosen to give the highest probability for fusion ignition for research purposes and was not optimized to produce net energy for fusion energy applications. Further improvements in yield are envisaged at NIF by further increasing laser energy and improving hohlraum efficiency [88] to drive larger targets [89] and by optimizing drive and capsule dopant profiles [90]. Inertial fusion energy (IFE) applications requiring advancements to the underlying scheme require further development, such as laser energy usage, shot rate, target robustness, higher fuel compression levels, and cost. However, the result reported herein demonstrates that it is possible to achieve a target gain greater than one in a laboratory scale system. As this letter was being finalized, several repeats of experiment N221204 were performed on NIF, shots N230729 and N230904, which achieved G_{target} of 1.9 and 1, respectively.

Appendix A: Historical summary of the ICF effort on NIF

Analysis of the first CH ablator [91] experiments up to about 2013 identified degradations from highly elevated levels of excess radiation loss resulting from mid to high-Z ablator material mixing into the fusing DT plasma [92]. Hydrodynamic instability was identified as the leading cause of mix [93]. A factor of ten improvement to the implosion quality was made by lowering the ablation front growth of capsule surface perturbations [94–98]; this resulted in a target gain of 0.015 and a fuel energy gain of $\gtrsim 1$ [99]. The "fuel energy gain," $G_{\text{fuel}} = Y_{\text{tot}}/E_{pdV}$, for ICF represents the ratio of total yield Y_{tot} (17.6 MeV per DT fusion) to the energy absorbed by the DT fuel and hot spot on compression, E_{pdV} [100, 101]. As alpha particles carry $1/5$ of the total fusion energy per D+T reaction, $G_{\text{fuel}} > 5$ marks heating dominated by alpha heating also known as the burning plasma regime. From 2013 to 2016, several new factors were identified as limiting the achievable fusion yield. These included additional hydrodynamic instabilities induced by the capsule surface quality and support tent [102–107], time dependent asymmetries [108–113] resulting in fuel areal density asymmetry that is a signature of wasted kinetic energy [114, 115] and laser plasma interactions (backscatter) decreasing the overall coupling [116–118]. Starting in 2014, two major developments occurred. First, the discovery that reducing gas fill in the hohlraum resulted in a great reduction in LPI effects [119], particularly the almost complete elimination of SRS scattered light and associated hot electrons, and a 15% increase in energy coupled to the capsule [120]. Second, material science research and implosion modeling [121] utilizing high density carbon (HDC) ablators [122, 123] began. Research in high-density low-Z ablators from 1995 to 1997 had laid the groundwork necessary for transitioning ablator materials. By 2016, the HDC design was shown in NIF experiments to overcome key limitations associated with plastic capsules [124–128]. The higher density of carbon ablators relative to plastic reduced the implosion time from 12 - 16 ns [129] down to 7 - 8 ns for similar design adiabat implosions. This reduced the amount of wall blow-in plasma filling the hohlraum, and combined with separating outer cones and beam spots within a quad [128, 130, 131] to reduce local intensities and hohlraum wall plasma ingress [53, 132] was synergistic with using lower hohlraum gas-fill, and improved time-dependent symmetry control [42, 133, 134]. By 2017 these improvements doubled the target gain (0.03) and gave fusion

yields exceeding the amount of energy coupled to the imploding HDC shell [135, 136]. Theory [74, 137] and detailed modeling [138] indicated that increasing the diameter of the HDC capsule by 10-20% while maintaining the implosion velocity, deceleration time, and symmetry could more than double the fusion yield moving towards the threshold of ignition [139]. Because implosion deceleration time was fixed, this strategy was not true "hydroscaling." The larger capsule designs reintroduced CBET, a key symmetry control capability first used in 2009 for high gas-fill hohlraums [140], to low gas-fill hohlraums [55], and varied hohlraum shape [141] as two methods for controlling implosion shape symmetry. In 2021, both methods resulted in a successful $\sim 3\times$ increase in the yield (~ 170 kJ) and a target gain of ~ 0.09. These implosions were also the first to achieve a burning plasma [142] in which the energy produced by alpha particle self-heating exceeded the inferred compressional work done to assemble the fuel.

Data, theory and modeling indicated that the yield of this series of implosions was being strongly impacted by a net hot spot translational velocity [36, 37, 143–148]. To help minimize this impact, three equatorial hohlraum diagnostic windows were repositioned to improve radiation drive symmetry [36, 149]. Additionally, observations and modeling indicated that additional radiative loss from high Z contaminant ablator material injected into the hot spot by the capsule DT fuel fill tube was a significant degradation to fusion yield and an inhibitor to ignition [39, 40, 150]. To mitigate this, the diameter of the capsule fill tube was reduced from 5 to 2 μm. To further reduce contaminant mix, the quality of the capsule was improved, with capsule surface pit and internal void characteristics reduced by an order of magnitude relative to the 2021 capsules to minimize the seeds for hydrodynamic mix [151].

In addition to these improvements, simulations showed quantitatively that the late-time ablation pressure could be further optimized by reducing the laser entrance hole (LEH) diameter from 3.65 to 3.1 mm without laser energy loss [152, 153], giving a 7% increase in radiation flux. X-ray drive power loss out of the LEHs scales as $\sigma T_r^4 A_{\text{LEH}}$ where σ is the Stefan-Boltzmann constant, A_{LEH} is the LEH area and T_r is the hohlraum radiation temperature [154, 155]. This extra efficiency was used to extend the duration of the laser pulse leading to a longer radiation drive and higher peak ablation pressure at late-time [23, 24, 156, 157], an effect understood to be essential to maximizing stagnation pressure in ICF implosions [114, 158]. These improvements together with improved target quality, led to a target gain of 0.72 and exceeding the Lawson criterion [22] on NIF shot N210808 on August 8, 2021.

Appendix B: NIF laser upgrades

Operating NIF at 2.05 MJ (351 nm), 440 TW peak power (8% energy increase compared to N210808) was made possible by two main improvements in the ultraviolet (UV) section of the NIF final optics assembly [48, 49]. First, a new fused silica debris shield was positioned between the grating debris shield (GDS) and the final disposable debris shield (DDS) on 128 beams. These new optics protect the GDS from the ejecta and debris generated by the laser from the DDS. Second, the installation of target chamber debris-blocking metal shields was deployed in strategic locations of the lower hemisphere beams. These shields significantly reduce the amount of target debris reaching the GDS. Both improvements enable NIF to operate for the first time at elevated energy (at fixed peak power) by limiting the GDS damage initiation and rate, and allow NIF to conduct target experiments at 2.05 MJ (351 nm), 440 TW peak power in a sustainable way within the maintenance capacity of the optic processing facilities. In parallel, the first modernization phase of the fiber-optics NIF front-end (known as Master Oscillator room) was completed in 12/2021 (after N210808) from the oscillators to the input of the pulse shaping systems. The upgrade consisted of redesigning and replacing fiber amplifiers, acousto-optic modulators, fail-safe systems to improve performance, mitigate obsolescence and increase ease of operation. Of note, the reported laser energies had to be corrected a few % downwards due to neutron background on the laser calorimeters. This modernization allowed more accurate and precise delivery of the NIF laser energy (shown in Fig.2) into the hohlraum.

Appendix C: Detailed capsule comparison between N210808 and N221204

Prior to target assembly, the HDC ablator surface, interior, and thickness uniformity are characterized. Holographic microscopy of the entire shell surface revealed a total of 70 surface pits on the N221204 capsule as compared to 269 surface pits on the capsule surface for the N210808 capsule. For both N221204 and N210808, no individual surface pit exceeded a volume of 3 μm^3. X-ray computed tomography over a 5% sample of the ablator volume revealed the presence of a single void ~ 2 μm^3 located 67μm below the ablator outer surface for N221204. The capsule for N210808 contained two voids of sizes 3 and 4 μm^3 located 50 and 72 μm, respectively, below the ablator surface. In contrast to prior experiments, the N221204 capsule contained a large number (> 400) of inclusions in its interior. The capsule for N210808 was found to contain 15 such inclusions. While the exact composition and volume of the inclusions has not been determined, fluorescence analysis shows that they are a sub-stoichiometric variation of tungsten carbide (less than one W atom per C atom). Better volume quan-

tification is still in process. Capsule wall thickness non-uniformity as measured by infrared thin film interference was < 0.2 μm ($< 0.25\%$ of the wall thickness). Apart from the large number of inclusions, the overall number of surface pits and internal voids in the N221204 abla-

tor was smaller than typical for high-energy NIF experiments. There were no significant differences in the cryogenic DT ice layer quality [159] between N210808 and N221204.

[1] N. A. of Sciences, *Biographical Memoirs: Volume 47* (The National Academies Press, Washington, DC, 1975).

[2] M. Bartusiak, *Archives of the universe : 100 discoveries that transformed our understanding of the cosmos*, first edition ed. (New York: Vintage Books, 2006).

[3] A. S. Eddington, Science **52**, 233 (1920).

[4] F. Aston, *Mass Spectra and Isotopes*, 1st ed. (Edward Arnold and Co., London, 1933).

[5] G. Gamow, Zeitschrift für Physik **51**, 204 (1928).

[6] Atkinson, R. d'E. and F. G. Houtermans, Zeitschrift für Physik **54**, 656 (1929).

[7] M. L. E. Oliphant, B. B. Kinsey, and E. Rutherford, Proceedings of the Royal Society of London. Series A, Containing Papers of a Mathematical and Physical Character **141**, 722 (1933).

[8] H. A. Bethe, Physical Review **55**, 434 (1939).

[9] J. D. Lawson, Proceedings of the Physical Society. Section B **70**, 6 (1957).

[10] J. P. Freidberg, *Plasma physics and fusion energy* (Cambridge university press, 2008).

[11] N. Basov and O. Krokhin, Sov. Phys. JETP **19**, 123 (1964).

[12] A. Kastler, C. R. Acad. Sci. **258**, 489 (1964).

[13] J. M. Dawson, The Physics of Fluids **7**, 981 (1964).

[14] J. Nuckolls, L. Wood, A. Thiessen, and G. Zimmerman, Nature **239**, 139 (1972).

[15] J. Lindl, Phys. Plasmas **2**, 3933 (1995).

[16] R. Craxton, K. Anderson, T. Boehly, V. Goncharov, D. Harding, J. Knauer, R. McCrory, P. McKenty, D. Meyerhofer, J. Myatt, *et al.*, Physics of Plasmas **22** (2015).

[17] S. A. Slutz and R. A. Vesey, Physical review letters **108**, 025003 (2012).

[18] E. M. Campbell and W. J. Hogan, Plasma Physics and Controlled Fusion **41**, B39 (1999).

[19] G. H. Miller, E. I. Moses, and C. R. Wuest, Nuclear Fusion **44**, S228 (2004).

[20] E. I. Moses, R. N. Boyd, B. A. Remington, C. J. Keane, and R. Al-Ayat, Phys. Plasmas **16**, 041006 (2009).

[21] M. L. Spaeth and et al., Fusion Science and Technology **69**, 25 (2017).

[22] H. Abu-Shawareb and et al. (Indirect Drive ICF Collaboration), Phys. Rev. Lett. **129**, 075001 (2022).

[23] A. Kritcher, A. Zylstra, D. Callahan, O. Hurricane, C. Weber, D. Clark, C. Young, J. Ralph, D. Casey, A. Pak, *et al.*, Physical Review E **106**, 025201 (2022).

[24] A. Zylstra, A. Kritcher, O. Hurricane, D. Callahan, J. Ralph, D. Casey, A. Pak, O. Landen, B. Bachmann, K. Baker, *et al.*, Physical Review E **106**, 025202 (2022).

[25] S. Haan, J. Lindl, D. Callahan, D. Clark, J. Salmonson, B. Hammel, L. Atherton, R. Cook, M. Edwards, S. Glenzer, *et al.*, Physics of Plasmas **18** (2011).

[26] S. E. Koonin *et al.* (National Academies Press, Washington, D.C., 1997) p. 64.

[27] A. Kritcher, A. Zylstra, C. Weber, O. Hurricane, *et al.*, Phys. Rev. E **X**, XXXXXX (2023).

[28] O. A. Hurricane *et al.*, Phys. Rev. Let. **X**, XXXXXX (2023).

[29] A. Pak, A. B. Zylstra, *et al.*, Phys. Rev. E **X**, XXXXXX (2023).

[30] S. H. Glenzer and et al., Phys. Plasmas **19**, 056318 (2012).

[31] M. J. Edwards and et al., Phys. Plasmas **20**, 070501 (2013).

[32] J. Lindl, O. Landen, J. Edwards, and E. Moses, Phys. Plasmas **21**, 020501 (2014).

[33] O. L. Landen and et al., Phys. Plasmas **18**, 051002 (2011).

[34] M. J. Edwards and et al., Phys. Plasmas **18**, 051003 (2011).

[35] A. Pak, L. Divol, D. Casey, S. Khan, A. Kritcher, J. Ralph, R. Tommasini, C. Trosseille, A. Zylstra, K. Baker, *et al.*, Physical Review Letters **131**, 065101 (2023).

[36] B. J. MacGowan and et al., High Energy Density Physics **40**, 100944 (2021).

[37] D. T. Casey and et al., Phys. Rev. Lett. **126**, 025002 (2021).

[38] IAEA, ed., Vol. XXXX (2023).

[39] A. Pak and et al., Phys. Rev. Lett. **124**, 145001 (2020).

[40] C. R. Weber and et al., Phys. Plasmas **27**, 032703 (2020).

[41] A. Pak, A. B. Zylstra, *et al.*, Phys. Rev. E **X**, XXXXX (2023).

[42] L. Divol and et al., Phys. Plasmas **24**, 056309 (2017).

[43] G. B. Zimmerman and W. L. Kruer, Comments on Plasma Physics and Controlled Fusion **2**, 51 (1975).

[44] M. M. Marinak and et al., Phys. Plasmas **3**, 2070 (1996).

[45] O. S. Jones and et al., Phys. Plasmas **19**, 056315 (2012).

[46] O. S. Jones and et al., Phys. Plasmas **24**, 056312 (2017).

[47] D. Strozzi, D. Bailey, P. Michel, L. Divol, S. Sepke, G. Kerbel, C. Thomas, J. Ralph, J. Moody, and M. Schneider, Physical Review Letters **118**, 025002 (2017).

[48] J. Di Nicola, T. Bond, M. Bowers, L. Chang, M. Hermann, R. House, T. Lewis, K. Manes, G. Mennerat, B. MacGowan, *et al.*, Nuclear Fusion **59**, 032004 (2018).

[49] J.-M. G. Di Nicola, T. Suratwala, L. Pelz, J. Heebner, D. Alessi, A. Bhasker, T. Bond, M. Bowers, G. Brunton, B. Buckley, *et al.*, in *High Power Lasers for Fusion Research VII* (SPIE, 2023) p. PC1240103.

[50] J. M. Di Nicola and et al., Nuclear Fusion **59**, 032004 (2019).

[51] S. H. Baxamusa, M. Stadermann, C. Aracne-Ruddle, A. J. Nelson, M. Chea, S. Li, K. Youngblood, and T. I. Suratwala, Langmuir **30**, 5126 (2014).

[52] D. A. Callahan, O. A. Hurricane, J. Ralph, and et al., Phys. Plasmas **25**, 056305 (2018).

[53] J. Ralph, O. Landen, L. Divol, A. Pak, T. Ma, D. Callahan, A. Kritcher, T. Döppner, D. Hinkel, C. Jarrott, *et al.*, Physics of Plasmas **25**, 102708 (2018).

[54] N. Izumi and et al., Phys. Plasmas **28**, 022706 (2021).

[55] A. L. Kritcher and et al., Phys. Rev. E **98**, 053206 (2018).

[56] K. Humbird *et al.*, Science **X**, XXXXXX (2023).

[57] T. Chapman and et al., Journal of Applied Physics **125**, 033101 (2019).

[58] J. Moody, P. Datte, K. Krauter, E. Bond, P. Michel, S. Glenzer, L. Divol, C. Niemann, L. Suter, N. Meezan, *et al.*, Review of Scientific Instruments **81** (2010).

[59] M. L. Spaeth, K. Manes, D. Kalantar, P. Miller, J. Heebner, E. Bliss, D. Spec, T. Parham, P. Whitman, P. Wegner, *et al.*, Fusion Science and Technology **69**, 25 (2016).

[60] M. D. Rosen, Phys. Plasmas **3**, 1803 (1996).

[61] J. D. Kilkenny and et al., Fusion Science and Technology **69**, 420 (2016).

[62] G. P. Grim and et al., Phys. Plasmas **20**, 056320 (2013).

[63] J. Frenje, R. Bionta, E. Bond, J. Caggiano, D. Casey, C. Cerjan, J. Edwards, M. Eckart, D. Fittinghoff, S. Friedrich, *et al.*, Nuclear Fusion **53**, 043014 (2013).

[64] M. Gatu Johnson and et al., Rev. Sci. Instrum. **85**, 11E104 (2014).

[65] V. Y. Glebov and et al., Rev. Sci. Instrum. **81**, 10D325 (2010).

[66] A. S. Moore and et al., Rev. Sci. Instrum. **94**, 061102 (2023).

[67] M. Gatu Johnson and et al., Rev. Sci. Instrum. **83**, 10D308 (2012).

[68] C. Yeamans and D. Bleuel, Fusion Science and Technology **72**, 120 (2017).

[69] J. Lindl, S. Haan, O. Landen, A. Christopherson, and R. Betti, Physics of Plasmas **25** (2018).

[70] D. Casey, J. Frenje, M. Gatu Johnson, F. Séguin, C. Li, R. Petrasso, V. Y. Glebov, J. Katz, J. Knauer, D. Meyerhofer, *et al.*, Review of Scientific Instruments **83**, 10D912 (2012).

[71] M. S. Rubery, M. Rosen, *et al.*, Phys. Rev. Lett. **X**, XXXXXX (2023).

[72] H.-S. Bosch and G. M. Hale, Nuclear Fusion **32**, 611 (1992).

[73] T. Murphy, Physics of Plasmas **21** (2014).

[74] O. Hurricane, D. Callahan, P. Springer, M. Edwards, P. Patel, K. Baker, D. Casey, L. Divol, T. Döppner, D. Hinkel, *et al.*, Plasma Physics and Controlled Fusion **61**, 014033 (2019).

[75] P. T. Springer and et al., Nuclear Fusion **59**, 32009 (2019).

[76] P. K. Patel, P. T. Springer, C. Weber, L. C. Jarrott, O. A. Hurricane, B. Bachmann, K. Baker, L. Berzak Hopkins, D. Callahan, D. T. Casey, *et al.*, Physics of Plasmas **27** (2020).

[77] R. Betti, K. Anderson, V. N. Goncharov, R. L. McCrory, D. D. Meyerhofer, S. Skupsky, and R. P. J. Town, Phys. Plasmas **9**, 2277 (2002).

[78] C. D. Zhou and R. Betti, Phys. Plasmas **16**, 079905 (2009).

[79] P. Y. Chang and et al., Phys. Rev. Lett. **104**, 135002 (2010).

[80] R. Betti and et al., Phys. Plasmas **17**, 058102 (2010).

[81] R. Betti, A. R. Christopherson, B. K. Spears, R. Nora, A. Bose, J. Howard, K. M. Woo, M. J. Edwards, and J. Sanz, Phys. Rev. Lett. **114**, 255003 (2015).

[82] A. R. Christopherson, R. Betti, A. Bose, J. Howard, K. M. Woo, E. M. Campbell, J. Sanz, and B. K. Spears, Phys. Plasmas **25**, 012703 (2018).

[83] O. A. Hurricane, S. A. Maclaren, M. Rosen, J. H. Hammer, P. T. Springer, and R. Betti, Phys. Plasmas **28**, 22704 (2021).

[84] O. Hurricane, P. Patel, R. Betti, D. Froula, S. Regan, S. Slutz, M. Gomez, and M. Sweeney, Reviews of Modern Physics **95**, 025005 (2023).

[85] S. E. Wurzel and S. C. Hsu, Phys. Plasmas **29**, 062103 (2022).

[86] A. B. Zylstra, R. Nora, P. K. Patel, and O. A. Hurricane, Phys. Plasmas **28**, 122703 (2021).

[87] L. Divol *et al.*, Physics of Plasmas **X**, XXXXX (2024).

[88] P. Amendt and et al., Phys. Plasmas **26**, 082707 (2019).

[89] A. Kritcher, A. Zylstra, D. Callahan, O. Hurricane, C. Weber, J. Ralph, D. Casey, A. Pak, K. Baker, B. Bachmann, *et al.*, Physics of Plasmas **28**, 072706 (2021).

[90] D. S. Clark and et al., Phys. Plasmas **29**, 052710 (2022).

[91] A. Nikroo and et al., Phys. Plasmas **13**, 056302 (2006).

[92] T. Ma and et al., Phys. Rev. Lett. **111**, 085004 (2013).

[93] V. A. Smalyuk and et al., Plasma Physics and Controlled Fusion **62**, 014007 (2020).

[94] T. R. Dittrich, O. Hurricane, and et al., Phys. Rev. Lett. **112**, 055002 (2014).

[95] D. T. Casey and et al., Phys. Rev. E **90**, 011102(R) (2014).

[96] K. Raman, V. Smalyuk, D. Casey, S. Haan, D. Hoover, O. Hurricane, J. Kroll, A. Nikroo, J. Peterson, B. Remington, *et al.*, Physics of Plasmas **21** (2014).

[97] O. A. Hurricane and et al., Phys. Plasmas **21**, 056314 (2014).

[98] A. G. MacPhee and et al., Phys. Plasmas **22**, 080702 (2015).

[99] O. A. Hurricane and et al., Nature **506**, 343 (2014).

[100] M. D. Rosen, Phys. Plasmas **6**, 1690 (1999).

[101] S. Atzeni and J. Meyer-ter Vehn, *The Physics of Inertial Fusion* (Oxford University Press, 2008).

[102] S. H. Baxamusa, M. Stadermann, C. Aracne-Ruddle, A. J. Nelson, M. Chea, S. Li, K. Youngblood, and T. I. Suratwala, Langmuir **30**, 5126 (2014).

[103] S. R. Nagel and et al., Phys. Plasmas **22**, 22704 (2015).

[104] R. Tommasini and et al., Phys. Plasmas **22**, 056315 (2015).

[105] D. S. Clark and et al., Phys. Plasmas **22**, 022703 (2015).

[106] B. A. Hammel, R. Tommasini, D. S. Clark, J. Field, M. Stadermann, and C. Weber, Journal of Physics: Conference Series **717**, 12021 (2016).

[107] J. E. Ralph and et al., Phys. Plasmas **27**, 102708 (2020).

[108] E. L. Dewald and et al., Phys. Rev. Lett. **111**, 235001 (2013).

[109] J. Moody, H. Robey, P. Celliers, D. Munro, D. Barker, K. Baker, T. Döppner, N. Hash, L. Berzak Hopkins, K. LaFortune, *et al.*, Physics of Plasmas **21**, 092702 (2014).

[110] J. R. Rygg and et al., Phys. Rev. Lett. **112**, 195001 (2014).

[111] R. P. J. Town and et al., Phys. Plasmas **21**, 056313 (2014).

[112] A. Kritcher, R. Town, D. Bradley, D. Clark, B. Spears, O. Jones, S. Haan, P. Springer, J. Lindl, R. Scott, *et al.*, Physics of Plasmas **21**, 042708 (2014).

[113] A. Pak and et al., Phys. Plasmas **24**, 056306 (2017).

[114] O. A. Hurricane, D. T. Casey, O. Landen, and et al., Physics of Plasmas **29**, 012703 (2022), https://doi.org/10.1063/5.0067699.

[115] K. M. Woo and R. Betti, Physics of Plasmas **28**, 054503 (2021), https://doi.org/10.1063/5.0045317.

[116] R. K. Kirkwood and et al., Phys. Plasmas **18**, 056311 (2011).

[117] J. L. Kline and et al., Phys. Plasmas **20**, 056314 (2013).

[118] J. Moody, D. Callahan, D. Hinkel, P. Amendt, K. Baker, D. Bradley, P. Celliers, E. Dewald, L. Divol, T. Döppner, *et al.*, Physics of Plasmas **21**, 056317 (2014).

[119] G. Hall, O. Jones, D. Strozzi, J. Moody, D. Turnbull, J. Ralph, P. Michel, M. Hohenberger, A. Moore, O. Landen, *et al.*, Physics of Plasmas **24** (2017).

[120] D. E. Hinkel and et al., Phys. Rev. Lett. **117**, 225002 (2016).

[121] D. D. M. Ho, S. W. Haan, J. D. Salmonson, D. S. Clark, J. D. Lindl, J. L. Milovich, C. A. Thomas, L. F. B. Hopkins, and N. B. Meezan, Journal of Physics: Conference Series **717**, 012023 (2016).

[122] J. Biener and et al., Nuclear Fusion **49**, 112001 (2009).

[123] T. Braun and et al., Nuclear Fusion **63**, 016022 (2023).

[124] A. J. MacKinnon and et al., Physics of Plasmas **21**, 056318 (2014).

[125] J. S. Ross and et al., Phys. Rev. E **91**, 021101 (2015).

[126] N. B. Meezan and et al., Phys. Plasmas **22**, 062703 (2015).

[127] L. F. Berzak Hopkins and et al., Phys. Rev. Lett. **114**, 175001 (2015).

[128] K. Baker, C. Thomas, D. Casey, S. Khan, B. Spears, R. Nora, T. Woods, J. Milovich, R. Berger, D. Strozzi, *et al.*, Physical review letters **121**, 135001 (2018).

[129] T. Döppner and et al., Phys. Plasmas **27**, 042701 (2020).

[130] P. Amendt, J. S. Ross, J. L. Milovich, M. Schneider, E. Storm, D. A. Callahan, D. Hinkel, B. Lasinski, D. Meeker, P. Michel, *et al.*, Physics of Plasmas **21** (2014).

[131] D. Casey, C. Thomas, K. Baker, B. Spears, M. Hohenberger, S. Khan, R. Nora, C. Weber, D. Woods, O. Hurricane, *et al.*, Physics of Plasmas **25** (2018).

[132] D. Callahan, O. Hurricane, J. Ralph, C. Thomas, K. Baker, L. Benedetti, L. Berzak Hopkins, D. Casey, T. Chapman, C. Czajka, *et al.*, Physics of Plasmas **25**, 056305 (2018).

[133] D. Turnbull and et al., Phys. Plasmas **23**, 052710 (2016).

[134] M. Hohenberger and et al., Phys. Plasmas **26**, 112707 (2019).

[135] L. Berzak Hopkins and et al., Plasma Physics and Controlled Fusion **61**, 014023 (2018).

[136] S. Le Pape and et al., Phys. Rev. Lett. **120**, 245003 (2018).

[137] R. Nora and et al., Phys. Plasmas **21**, 056316 (2014).

[138] D. S. Clark and et al., Phys. Plasmas **26**, 050601 (2019).

[139] O. A. Hurricane and et al., Physics of Plasmas **26**, 052704 (2019), https://doi.org/10.1063/1.5087256.

[140] P. Michel and et al., Phys. Rev. Lett. **102**, 25004 (2009).

[141] H. F. Robey, L. Berzak Hopkins, J. L. Milovich, and N. B. Meezan, Phys. Plasmas **25**, 012711 (2018).

[142] A. B. Zylstra, O. A. Hurricane, *et al.*, Nature **601**, 542 (2022).

[143] B. K. Spears and et al., Phys. Plasmas **21**, 042702 (2014).

[144] H. G. Rinderknecht, D. T. Casey, R. Hatarik, R. M. Bionta, B. J. MacGowan, P. Patel, O. L. Landen, E. P. Hartouni, and O. A. Hurricane, Phys. Rev. Lett. **124**, 145002 (2020).

[145] O. A. Hurricane, D. T. Casey, and et al., Phys. Plasmas **27**, 062704 (2020).

[146] C. V. Young, L. Masse, D. T. Casey, B. J. MacGowan, O. L. Landen, D. A. Callahan, N. B. Meezan, R. Nora, and P. K. Patel, Phys. Plasmas **27** (2020).

[147] D. J. Schlossberg and et al., Phys. Rev. Lett. **127**, 125001 (2021).

[148] J. L. Milovich and et al., Plasma Physics and Controlled Fusion **63**, 025012 (2021).

[149] K. L. Baker, P. A. Amendt, J. S. Ross, V. Smalyuk, O. L. Landen, D. D. Ho, S. Khan, S. W. Haan, J. D. Lindl, D. Mariscal, *et al.*, Physics of Plasmas **30**, 092708 (2023).

[150] B. Bachmann and et al., Phys. Rev. E **101**, 033205 (2020).

[151] A. Zylstra and et al., Phys. Plasmas **27**, 092709 (2020).

[152] M. B. Schneider and et al., Phys. Plasmas **22**, 122705 (2015).

[153] S. A. MacLaren and et al., Phys. Rev. Lett. **112**, 105003 (2014).

[154] L. J. Suter and et al., Phys. Plasmas **3**, 2057 (1996).

[155] R. L. Kauffman and et al., Phys. Rev. Lett. **73**, 2320 (1994).

[156] O. L. Landen and et al., Plasma Physics and Controlled Fusion **54**, 124026 (2012).

[157] V. A. Smalyuk and et al., Phys. Rev. Lett. **111**, 215001 (2013).

[158] O. A. Hurricane, A. Kritcher, D. A. Callahan, O. L. Landen, and et al., Phys. Plasmas **24**, 092706 (2017).

[159] J. A. Koch and et al., Fusion Science and Technology **55**, 244 (2009).